Asian J Biol Life Sci., 2026; 15(2):353-365.
https://ajbls.com

Research Article

Molecular Docking and ADMET Profiling of Hydantoin Derivatives Targeting Voltage-Gated Sodium Channel (PDB ID: 1N45) for Epilepsy Treatment

Shankesh Sanjay Bhure[1], Rohit Jaysing Bhor[1,*], Amol Mohan Shirode[2], Harshali Narayan Anap[3], Pravin Bapurao Jadhav[4], Apurva Ranganath Gosavi[5], Anuj Vishnu Algude[5]

[1]Department of Pharmaceutical Chemistry, Pravara Rural College of Pharmacy Pravaranagar, Tal-Rahata, Ahmednagar, Maharashtra, INDIA.
[2]Department of Pharmaceutical Chemistry, K. B. H. S. S. Trust Institute of Pharmacy Malegaon, District Nashik, Maharashtra, INDIA.
[3]Department of Pharmaceutical Chemistry, Sitabai Thite college of Pharmacy, Shirur, Pune, Maharashtra, INDIA.
[4]Department of Pharmaceutical Chemistry, Sandip Institute of Pharmaceutical sciences, Nashik, Maharashtra, INDIA.
[5]Department of Pharmaceutical Chemistry, Pravara Rural College of Pharmacy Pravaranagar, Tal-Rahata, Ahmednagar, Maharashtra, INDIA.

ABSTRACT

Introduction: Epilepsy is a chronic neurological disorder characterized by recurrent seizures resulting from abnormal neuronal excitability, often associated with dysfunction of voltage-gated sodium channels. The present study aims to design and evaluate novel hydantoin-based derivatives of Phenytoin (PHT) as potential anticonvulsant agents using comprehensive *in silico* approaches. **Materials and Methods:** A series of ten derivatives (SB-1 to SB-10) were designed and assessed for their physicochemical properties, pharmacokinetic behavior, drug-likeness, toxicity profile, and molecular docking interactions with the voltage-gated sodium channel protein (PDB ID: 1N45). **Results:** Physicochemical analysis demonstrated that most compounds possess favorable drug-like characteristics, including optimal lipophilicity and acceptable topological polar surface area, supporting good membrane permeability. ADME predictions revealed high gastrointestinal absorption and blood-brain barrier permeability for selected derivatives, indicating their potential for central nervous system activity. **Discussion:** Toxicity assessments suggested low cardiotoxicity and minimal clinical toxicity risk, although moderate mutagenicity was observed in a few compounds, necessitating further validation. Molecular docking studies showed strong binding affinities across all derivatives, with docking scores ranging from -7.5 to -9.5 kcal/mol. Among the series, SB-3 exhibited the highest binding affinity, supported by diverse interactions including electrostatic, hydrophobic, and π-mediated interactions, while SB-8 and SB-9 also demonstrated significant binding stability through multiple hydrogen bonds. **Conclusion:** The integrated computational findings highlight SB-3 as a promising lead compound, with SB-8 and SB-9 as potential candidates for further development. This study provides valuable insights into the rational design of novel anticonvulsant agents targeting sodium channels and establishes a foundation for future experimental validation and optimization.

Keywords: Anticonvulsant activity, Blood-brain barrier, Drug-likeness, Epilepsy, Hydantoin derivatives, Molecular docking, Voltage-gated sodium channel.

Correspondence:
Dr. Rohit Jaysing Bhor
Department of Pharmaceutical Chemistry, Pravara Rural College of Pharmacy Pravaranagar, Tal-Rahata, Ahmednagar, Maharashtra, INDIA.
Email: rohit.bhor69@gmail.com
ORCID: 0000-0002-7979-3765
Web of Science Researcher ID: GMX-4028-2022

Received: 28-04-2026;
Revised: 11-06-2026;
Accepted: 09-07-2026.

INTRODUCTION

Brain disorders comprise a broad spectrum of neurological conditions that affect the structure, function, and biochemical balance of the central nervous system (Acharjee *et al.*, 2021). These disorders may arise from genetic abnormalities, traumatic brain injury, infections, metabolic disturbances, vascular insults, or neurodegenerative processes (Benet *et al.*, 2016). As the brain regulates cognition, behavior, sensation, and motor coordination, disturbances in neural circuitry can result in significant functional impairment and reduced quality of life (Berman *et al.*, 2000). Neurological brain disorders include epilepsy, Alzheimer's disease, Parkinson's disease, stroke, and multiple sclerosis, among others. Among these conditions, epilepsy represents one of the most prevalent chronic neurological disorders worldwide (Brodie *et al.*, 1996). Epilepsy is a chronic, non-communicable brain disorder characterized by a persistent predisposition to generate recurrent, unprovoked seizures. According to the World Health Organization, epilepsy affects millions of individuals globally and contributes substantially to neurological morbidity, disability, and social stigma (Chen *et al.*, 1994). A seizure is defined as a transient occurrence of signs and/or symptoms

OPEN ACCESS
Manuscript TECHNOMEDIA

DOI: 10.5530/ajbls.20260138

resulting from abnormal, excessive, and synchronous neuronal activity in the brain. The pathophysiology of epilepsy involves an imbalance between excitatory and inhibitory neurotransmission, primarily mediated by glutamate and Gamma-Aminobutyric Acid (GABA), leading to neuronal hyperexcitability and hypersynchronization (DiMasi *et al*., 2016). Seizures are broadly classified into focal seizures, originating within networks limited to one cerebral hemisphere, and generalized seizures, which involve bilateral neural networks from onset. The etiology of epilepsy is multifactorial and may include genetic mutations, structural brain lesions, tumors, stroke, central nervous system infections, and developmental abnormalities (Ekins *et al*., 2007). However, in a significant proportion of cases, the underlying cause remains idiopathic. Despite advances in neuroimaging, electrophysiological diagnostics such as Electroencephalography (EEG), and pharmacotherapy, epilepsy continues to impose a considerable healthcare burden. Approximately two-thirds of patients achieve seizure control with anti-epileptic drugs, while the remaining individuals may develop drug-resistant epilepsy requiring surgical or neuromodulatory interventions (Ghose *et al*., 1999). Ongoing research focuses on molecular mechanisms, novel therapeutic targets, and precision medicine approaches to improve disease management and patient outcomes (Gleeson *et al*., 2008). PDB ID: 1N45 corresponds to a structural domain of a voltage-gated sodium channel (Nav channel). Voltage-gated sodium channels are essential membrane proteins responsible for the initiation and propagation of action potentials in neurons (Gohlke *et al*., 2002). These channels play a critical role in neuronal excitability, and dysfunction in sodium channel activity is strongly associated with epilepsy. Mutations in sodium channel genes such as SCN1A, SCN2A, and SCN8A are well documented in epileptic syndromes (Goodford *et al*., 1985). Protein 1N45 (Protein Data Bank ID) represents a crystallographic structure of a voltage-gated sodium channel (Nav channel) domain, a transmembrane ion channel involved in the initiation and propagation of neuronal action potentials (Hevner *et al*., 2016). Voltage-gated sodium channels are integral membrane proteins composed of α-subunits forming the ion-conducting pore and auxiliary β-subunits that regulate gating properties. Nav channels are essential for rapid depolarization in excitable tissues, particularly neurons (Hopkins *et al*., 2008). Dysregulation or mutation in sodium channel genes (SCN1A, SCN2A, SCN8A) has been strongly implicated in epileptic syndromes, including generalized epilepsy and epileptic encephalopathies. Excessive sodium influx results in neuronal hyperexcitability, which is the core pathophysiological mechanism underlying seizure generation (Jorgensen *et al*., 2004). The comprehensive *in silico* evaluation of PHT derivatives demonstrated favorable physicochemical, pharmacokinetic, drug-likeness, and safety characteristics (Kwan *et al*., 2000). Analysis of hydrogen bonding capacity revealed acceptable numbers of hydrogen bond donors and acceptors across the series, supporting good membrane permeability and oral absorption potential (Lipinski *et al*., 1997). The TPSA values of most derivatives remained within the optimal range for intestinal absorption (<140 Å^2), although compounds with elevated TPSA showed comparatively reduced permeability predictions. (Lipinski *et al*., 2004) Lipophilicity indices (iLOGP, XLOGP3, and WLOGP) were within acceptable limits for the majority of compounds, indicating a balanced hydrophilic-lipophilic profile essential for drug-like behavior. ADME predictions indicated predominantly high gastrointestinal absorption and favorable BBB permeability for selected derivatives, suggesting potential systemic and central nervous system activity (Lionta *et al*., 2014). None of the compounds were predicted to be P-glycoprotein substrates, implying reduced efflux liability. However, inhibition of certain CYP450 isoforms (notably CYP2C19 and CYP2C9) was observed across the series, indicating the need for further metabolic interaction studies (Morris *et al*., 2009). Drug-likeness assessment demonstrated strong compliance with Lipinski, Veber, and Egan rules for most derivatives, with acceptable bioavailability scores (0.55) in the majority of compounds. A few derivatives exhibited rule violations and lower predicted bioavailability (0.17), suggesting possible structural optimization requirements. Toxicity prediction analysis revealed low cardiotoxicity risk across the series (Ng *et al*., 2003). Most compounds were predicted to be non-mutagenic and exhibited minimal clinical toxicity risk. Additionally, the derivatives showed negligible predicted interaction with GABA receptors and voltage-gated sodium channels, indicating a low probability of neurotoxicity or ion channel-related adverse effects (O'Boyle *et al*., 2011).

MATERIALS AND METHODS

Materials

The link between the target receptor, the anticipated lead chemical molecule, and its protein receptors is often investigated using docking in modern drug research. The study was conducted electronically using computational techniques (Pardridge *et al*., 2005). Discovery Studio (https://discover.3ds.com/discovery-studio-visualizer-download) was used to display the (2D) (3D) images. ADMET Prediction *in silico* to forecast their pharmacokinetic profiles, the best medications selected from molecular docking studies were evaluated for ADME characteristics (Pires *et al*., 2015). The sketch tool in Discovery Studio is used to create the molecules in two and three dimensions. The compound was created in Marvin Sketch, optimized in three dimensions, and saved in SDF format.

Methods

Protein Preparation

The three-dimensional crystal structure of human aromatase complexed with an inhibitor (PDB ID: 1N45) was provided by the RCSB Protein Data Bank with https://www.rcsb.org/ mention in

Figure 1. Several pre-processing steps were carried out to prepare the protein structure for molecular docking analysis (Rogers *et al.*, 2010). These included assigning bond orders, adding and removing hydrogen atoms as needed, forming zero-order metal bonds, and completing missing side chains and loops using Prime. Water molecules located more than 5 Å away from hetero groups were also removed to reduce unnecessary interactions (Santos *et al.*, 2017). Following the initial preparation, the protein structure was further refined through ionization, protonation, and charge correction to better mimic physiological conditions. Missing hydrogen atoms were added to stabilize the structure, and energy minimization was conducted to relieve steric clashes (Sliwoski *et al.*, 2014). The final optimization of the protein was performed using Swiss-PDB Viewer**,** ensuring a stable and energetically favorable conformation for subsequent docking studies.

Preparation of ligand

5,5-diphenylimidazolidine-2,4-dione and its substituted scaffolds were used as ligands mention in Table 1 for the docking study. For chemical structures, Chem Draw was used to sketch, which were then converted into three-dimensional structures (Trott *et al.*, 2010). Ligands were prepared by using Schrodinger's Lig Prep module (Table 1). The ligands' overall energy-minimized Potential of stereoisomers were kept, and the refined ligands were stored in Maestro format (Veber *et al.*, 2002).

RESULTS

Physicochemical properties of the designed PHT derivatives

The physicochemical properties of the designed PHT derivatives (SB-1 to SB-10) were evaluated to assess their drug-likeness and oral bioavailability potential (Table 2). Key parameters analysed included Hydrogen Bond Acceptors (HBA), Hydrogen Bond Donors (HBD), Molar Refractivity (MR), Topological Polar Surface Area (TPSA), and lipophilicity indices (iLOGP, XLOGP3, and WLOGP). All derivatives exhibited 1 hydrogen bond donor, while hydrogen bond acceptors ranged from 3 to 7. Compounds SB-1 to SB-5 and SB-7 contained 3 HBA, SB-8 to SB-10 contained 5 HBA, and SB-6 showed the highest number (7 HBA), indicating comparatively higher polarity. The Molar Refractivity (MR) values ranged from 130.52 (SB-7) to 153.98 (SB-6), suggesting acceptable molecular volume and polarizability across all compounds. Most compounds (SB-1 to SB-5, SB-7) exhibited similar MR values (~136-144), indicating structural similarity within this subset. The TPSA values revealed two distinct groups. SB-1 to SB-5 and SB-7 showed TPSA of 61.77 Å², which is favorable for good membrane permeability and oral absorption. SB-8, SB-9, and SB-10 demonstrated moderate TPSA (107.59 Å²), while SB-6 showed the highest TPSA (153.41 Å²), suggesting comparatively reduced membrane permeability. Lipophilicity analysis indicated iLOGP values between 2.96 and 4.12, XLOGP3 values between 4.66 and 5.83, and WLOGP values between 4.04 and 5.33. SB-5 exhibited the highest lipophilicity among the series, whereas SB-6 showed relatively lower lipophilicity. Most compounds fall within acceptable lipophilicity ranges for drug candidates, supporting their potential for oral bioavailability. The majority of PHT derivatives comply with Lipinski's Rule of Five, demonstrating acceptable hydrogen bonding capacity and lipophilicity. Compounds SB-1 to SB-5 and SB-7 appear particularly promising due to balanced polarity (TPSA < 90 Å²) and moderate lipophilicity. In contrast, SB-6 may exhibit reduced permeability due to its high TPSA and increased polarity (Figure 2).

ADME and Pharmacokinetic Prediction of PHT Derivatives

The pharmacokinetic profile of the designed PHT derivatives (SB-1 to SB-10) was evaluated using *in silico* ADME prediction parameters, including Gastrointestinal (GI) absorption, Blood-Brain Barrier (BBB) permeability, P-glycoprotein (P-gp) substrate prediction, and Cytochrome P450 (CYP) enzyme inhibition potential. Most derivatives demonstrated high GI absorption, indicating favorable oral bioavailability (Table 3). Compounds SB-1 to SB-5, SB-7, SB-8, SB-9, and SB-10 were predicted to possess high absorption, suggesting efficient intestinal permeability. In contrast, SB-6 exhibited low GI absorption, which may be attributed to its higher polarity and elevated TPSA observed in physicochemical analysis. BBB permeability prediction revealed that SB-1 to SB-5 and SB-7 are BBB permeant, suggesting potential Central Nervous System (CNS) activity. Conversely, SB-6, SB-8, SB-9, and SB-10 were predicted as non-permeant, indicating limited CNS exposure.

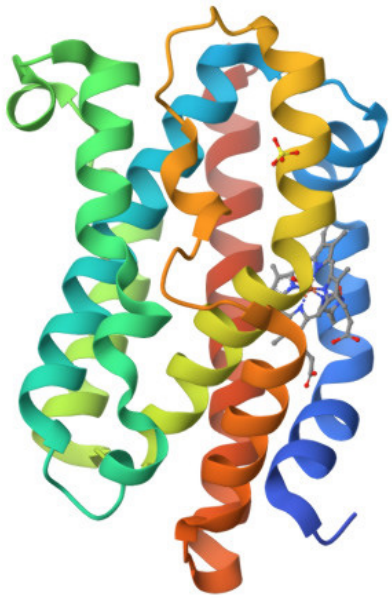

Figure 1: Crystal structure of x-ray crystal structure of human heme oxygenase-1 (ho-1) in complex with its substrate heme of 1N45 | pdb_00001n45.

Table 1: 5,5-diphenylimidazolidine-2,4-dione (Hydantoin), and its substituted derivative from SB1-SB10.

PHT Derivatives	Structure	PHT Derivatives	Structure
SB-1	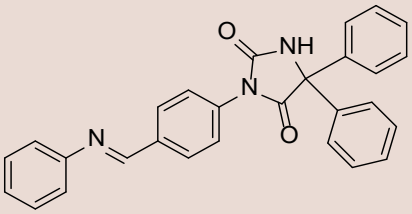	SB-6	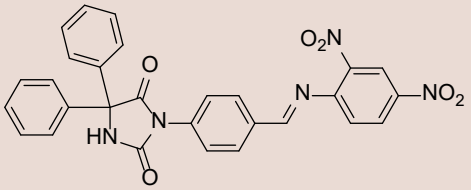
SB-2	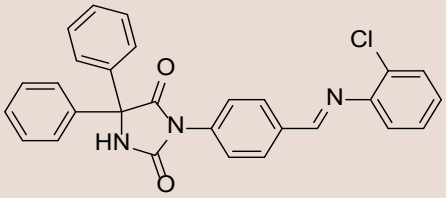	SB-7	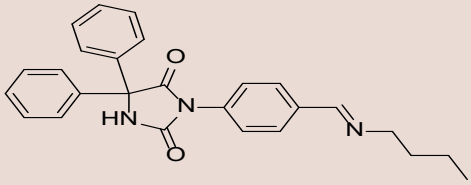
SB-3	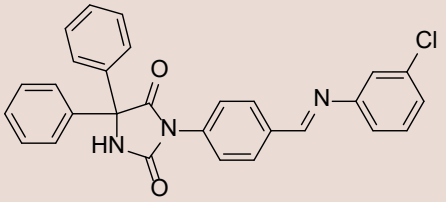	SB-8	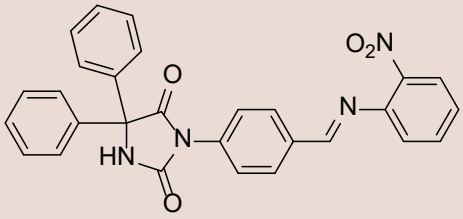
SB-4	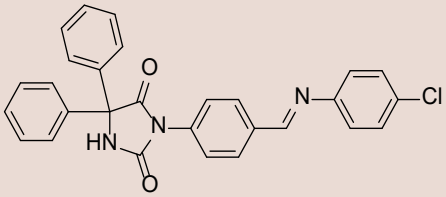	SB-9	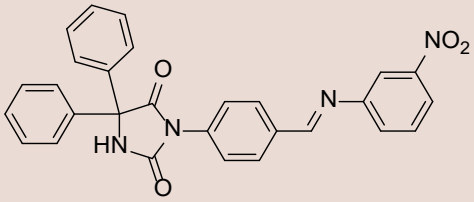
SB-5	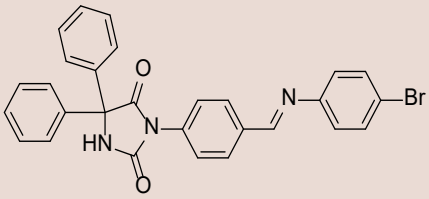	SB-10	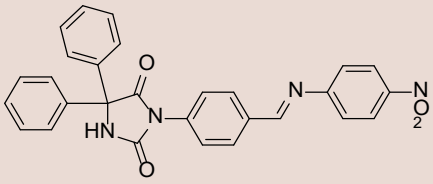

This distinction may be influenced by differences in polarity and lipophilicity among the derivatives. All compounds were predicted as non-substrates of P-gp, suggesting a lower likelihood of active efflux by membrane transporters. This characteristic supports improved intracellular retention and bioavailability. CYP3A4 inhibition varied within the series. SB-1, SB-6, SB-7, SB-8, SB-9, and SB-10 were predicted to inhibit CYP3A4, while SB-2, SB-3, SB-4, and SB-5 showed no inhibition of this enzyme. Collectively, the majority of PHT derivatives exhibit favorable pharmacokinetic characteristics, including high GI absorption and absence of P-gp substrate behavior. Compounds SB-1 to SB-5 and SB-7 demonstrate an optimal balance of oral absorption and BBB permeability. However, consistent inhibition of CYP2C19 and CYP2C9 across the series suggests the need for careful metabolic and drug-drug interaction evaluation in further experimental studies. SB-6 appears comparatively less favorable due to low GI absorption and lack of BBB permeability, likely associated with its higher polarity. Compounds SB-2 to SB-5 may represent the most balanced pharmacokinetic profiles due to high absorption, BBB permeability, absence of P-gp substrate liability, and lack of CYP3A4 inhibition.

Drug-Likeness Rule Evaluation

The drug-likeness of PHT derivatives (SB-1 to SB-10) was assessed using Lipinski, Ghose, Veber, Egan, and Muegge filters along with bioavailability score prediction. Compounds SB-1 to SB-4, SB-7, SB-8, SB-9, and SB-10 exhibited zero Lipinski violations, indicating compliance with the Rule of Five and favorable oral drug-like characteristics. In contrast, SB-5 and SB-6 showed two Lipinski violations, suggesting possible limitations in permeability or molecular properties. According to the Ghose filter, most compounds displayed one violation,

whereas SB-5 and SB-6 exhibited two violations, indicating slight deviations in molecular weight, molar refractivity, or lipophilicity parameters. Importantly, Veber and Egan rules were satisfied by most derivatives, except SB-6, which showed one violation each, potentially due to higher polarity and TPSA. Muegge analysis revealed minimal violations across the series. Notably, SB-7 to SB-10 showed no Muegge violations, suggesting an optimal balance of physicochemical properties. The bioavailability score further supported these findings. SB-1 to SB-4 and SB-7 to SB-10 demonstrated a predicted bioavailability score of 0.55, indicating good oral bioavailability potential. Conversely, SB-5 and SB-6 showed a reduced score of 0.17, correlating with their multiple rule violations. The SB-1 to SB-4 and SB-7 to SB-10 exhibited strong drug-likeness profiles, while SB-5 and SB-6 may require structural optimization (Table 4).

In silico Toxicity and Safety Profile

Toxicological predictions were performed to evaluate cardiotoxicity, mutagenicity, BBB penetration, clinical toxicity, GABA receptor interaction, and Voltage-Gated Sodium (VG Na^+) channel inhibition. All compounds were predicted as inactive (I) for cardiotoxicity with high probability scores (0.86-0.93), suggesting low risk of cardiac adverse effects. SB-1 to SB-5 and SB-7 were predicted inactive for mutagenicity, whereas SB-6, SB-8, SB-9, and SB-10 showed Active (A) predictions with moderate probability scores (~0.79-0.80), indicating potential genotoxic liability requiring experimental validation (Table 5). Most derivatives (SB-1 to SB-5, SB-7) were predicted as BBB permeable (A), supporting CNS penetration potential. SB-6, SB-8, SB-9, and SB-10 demonstrated comparatively lower BBB penetration probabilities. The majority of compounds were predicted inactive for clinical toxicity with acceptable probability values. No compound showed high predicted clinical toxicity risk. All derivatives were predicted inactive for GABA receptor modulation and voltage-gated sodium channel inhibition, indicating minimal risk of neurotoxicity or ion-channel-related adverse effects.

Binding interactions between the ligand and the active site residues of the target protein

The presented Table 5 containing diagram illustrates the binding interactions between the ligand and the active site residues of the

Table 2: Physicochemical properties of the designed PHT derivatives including #H-bond acceptors; #H-bond donors; MR; TPSA; iLOGP; XLOGP3; WLOGP.

PHT Derivatives	#H-bond acceptors	#H-bond donors	MR	TPSA	iLOGP	XLOGP3	WLOGP
SB-1	3	1	136.34	61.77	3.68	5.14	4.57
SB-2	3	1	141.35	61.77	4.01	5.8	5.22
SB-3	3	1	141.35	61.77	3.9	5.8	5.22
SB-4	3	1	141.35	61.77	4.02	5.77	5.22
SB-5	3	1	144.04	61.77	4.12	5.83	5.33
SB-6	7	1	153.98	153.41	2.96	4.83	4.38
SB-7	3	1	130.52	61.77	4.07	4.66	4.04
SB-8	5	1	145.16	107.59	3.47	5	4.48
SB-9	5	1	145.16	107.59	3.55	5	4.48
SB-10	5	1	145.16	107.59	3.48	4.97	4.48

Table 3: Comparative Analysis of Pharmacokinetic and ADME Properties.

PHT Derivatives	GI absorption	BBB permeant	Pgp substrate	CYP1A2 inhibitor	CYP2C19 inhibitor	CYP2C9 inhibitor	CYP2D6 inhibitor	CYP3A4 inhibitor
SB-1	High	Yes	No	No	Yes	Yes	No	Yes
SB-2	High	Yes	No	No	Yes	Yes	No	No
SB-3	High	Yes	No	No	Yes	Yes	No	No
SB-4	High	Yes	No	No	Yes	Yes	No	No
SB-5	High	Yes	No	No	Yes	Yes	No	No
SB-6	Low	No	No	No	Yes	Yes	No	Yes
SB-7	High	Yes	No	No	Yes	Yes	No	Yes
SB-8	High	No	No	No	Yes	Yes	No	Yes
SB-9	High	No	No	No	Yes	Yes	No	Yes
SB-10	High	No	No	No	Yes	Yes	No	Yes

Table 4: Comparative Analysis of Pharmacokinetic and ADME Properties.

PHT Derivatives	Lipinski #violations	Ghose #violations	Veber #violations	Egan #violations	Muegge #violations	Bioavailability Score
SB-1	0	1	0	0	1	0.55
SB-2	0	1	0	0	1	0.55
SB-3	0	1	0	0	1	0.55
SB-4	0	1	0	0	1	0.55
SB-5	2	2	0	0	1	0.17
SB-6	2	2	1	1	1	0.17
SB-7	0	1	0	0	0	0.55
SB-8	0	1	0	0	0	0.55
SB-9	0	1	0	0	0	0.55
SB-10	0	1	0	0	0	0.55

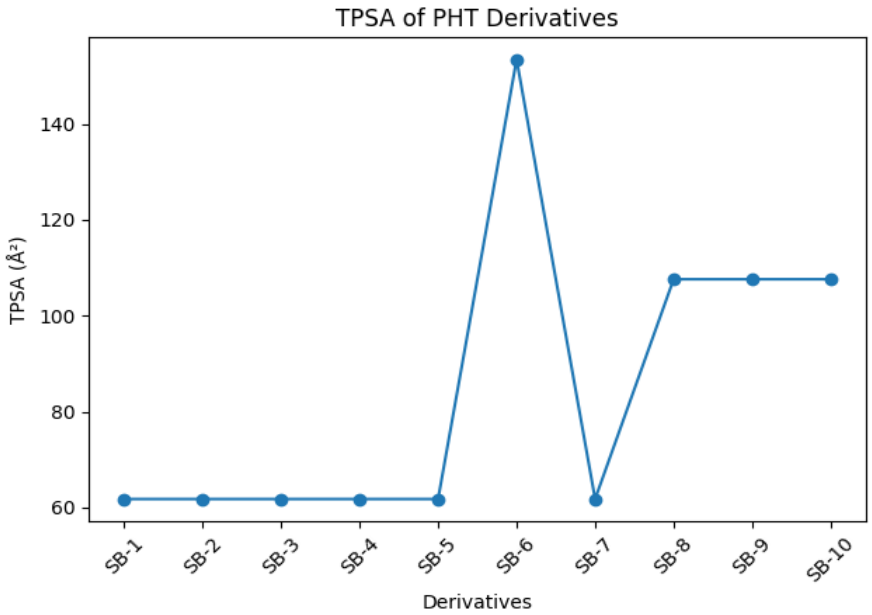

Figure 2: Physicochemical properties of the designed PHT derivatives including TPSA graph.

target protein. The ligand is shown at the center in a ball-and-stick format, while the surrounding amino acid residues are represented as labeled nodes forming the binding pocket. Hydrogen bonds are indicated by green dashed lines, demonstrating strong and specific interactions between the ligand heteroatoms (such as N or O) and key amino acid residues. These interactions play a crucial role in ligand stabilization and binding specificity within the active site. Several surrounding residues contribute to hydrophobic contacts, shown by light green or gray shaded regions. These interactions enhance binding affinity by stabilizing the ligand through van der Waals forces and nonpolar contacts. Aromatic rings of the ligand participate in π-π stacking or π-alkyl interactions with aromatic or hydrophobic residues (Table 6). These interactions are essential for anchoring the ligand inside the binding cavity and improving docking scores. Polar residues around the ligand contribute to electrostatic and dipole-dipole interactions, further strengthening ligand-protein association. The circular arrangement of residues indicates that the ligand is well-embedded within the active site cavity, suggesting good shape complementarity and favorable orientation for biological activity. The interaction map demonstrates that the ligand forms multiple stabilizing interactions, including hydrogen bonds and hydrophobic contacts, with critical amino acid residues of the target protein. This interaction profile supports the high docking score and predicted binding affinity, indicating that the ligand is a promising candidate for further biological evaluation.

Molecular Docking Analysis of PHT Derivatives

The binding interactions of PHT derivatives (SB-1 to SB-10) with the active site of the target protein were evaluated through molecular docking analysis. Docking scores ranged from -7.5 to -9.5 kcal/mol, indicating favorable binding affinities across the series (Table 7). The interaction profiles revealed a combination of hydrogen bonding, hydrophobic, electrostatic, and π-mediated

interactions contributing to ligand stabilization within the binding pocket. Among the evaluated derivatives, SB-3 exhibited the strongest binding affinity with a docking score of -9.5 kcal/mol, followed by SB-9 (-8.9 kcal/mol) and SB-8 (-8.8 kcal/mol). SB-4 demonstrated a score of -8.7 kcal/mol, while SB-1, SB-5, and SB-7 showed comparable affinities (-8.4 kcal/mol). SB-2 and SB-6 exhibited slightly lower binding energies (-8.2 kcal/mol), and SB-10 displayed the least binding affinity (-7.5 kcal/mol). Hydrogen bonding played a critical role in ligand stabilization with Several compounds (SB-1, SB-2, SB-6, SB-7, and SB-10) formed conventional hydrogen bonds with THR168, with bond distances ranging from 2.30 to 2.77 Å, indicating strong interactions. SB-7 formed multiple hydrogen bonds involving THR168 and ARG44, strengthening its binding stability. SB-8 and SB-9 formed dual hydrogen bonds with ARG44, with short bond distances (~2.3-2.6 Å), enhancing binding affinity. SB-4 showed a carbon hydrogen bond interaction with PHE95. Hydrophobic interactions were widely observed, particularly involving residues such as: PHE95; PRO158; LYS148; ALA175; LEU147; VAL146; MET34; TRP96. SB-3 demonstrated the most diverse interaction profile, including electrostatic (Pi-Cation), hydrophobic (Pi-Alkyl), Pi-Sulfur, and multiple aromatic stacking interactions, which likely contributed to its superior docking score. The docking analysis demonstrates that all PHT derivatives bind effectively within the active site of the target protein. SB-3 emerged as the most promising candidate, exhibiting the strongest binding affinity and diverse stabilizing interactions. Compounds SB-8 and SB-9 also showed strong binding profiles supported by multiple hydrogen bonds and hydrophobic contacts (Figure 3).

DISCUSSION

The present study provides a detailed *in silico* evaluation of Phenytoin (PHT) derivatives (SB-1 to SB-10) targeting the voltage-gated sodium channel protein (PDB ID: 1N45), which plays a crucial role in neuronal excitability and seizure propagation. The integration of physicochemical analysis, pharmacokinetic profiling, toxicity prediction, and molecular docking offers a holistic understanding of the therapeutic potential of these derivatives as anticonvulsant agents. The physicochemical properties of the designed compounds indicate that the majority of derivatives possess favorable drug-like characteristics. Hydrogen Bond Donor (HBD) and Acceptor (HBA) values fall within acceptable limits, ensuring optimal interaction capability with biological targets. Compounds SB-1 to SB-5 and SB-7, in particular, demonstrated balanced topological polar surface area (TPSA ~61.77 Å²), which is strongly associated with efficient membrane permeability and oral absorption. In contrast, SB-6 exhibited significantly higher TPSA (153.41 Å²), suggesting reduced permeability, which is consistent with its lower gastrointestinal absorption observed in ADME predictions. Lipophilicity values (iLOGP, XLOGP3, WLOGP) were within acceptable ranges for most derivatives, indicating an appropriate balance between hydrophilicity and lipophilicity, a key determinant of bioavailability. The ADME (Absorption, Distribution, Metabolism, and Excretion) analysis further supports the drug-likeness of the compounds. Most derivatives demonstrated high gastrointestinal absorption, suggesting good oral bioavailability. Importantly, compounds SB-1 to SB-5 and SB-7 showed Blood-Brain Barrier (BBB) permeability, which is essential for Central Nervous System (CNS)-active drugs such as anticonvulsants. The absence of P-glycoprotein substrate characteristics across all derivatives indicates a reduced likelihood of efflux-mediated drug resistance, enhancing their therapeutic potential. However, the consistent inhibition of CYP2C19 and CYP2C9 enzymes across the series raises concerns regarding potential drug-drug interactions and metabolic liabilities. Compounds SB-2 to SB-5 stand out as promising candidates due to their balanced pharmacokinetic profiles, including high absorption, BBB permeability, and lack of CYP3A4 inhibition. In contrast, SB-6 exhibited suboptimal ADME properties, likely due to its increased polarity. Drug-likeness evaluation using multiple rule-based filters (Lipinski, Ghose, Veber, Egan, and Muegge)

Table 5: Comparative Toxicity and ADMET Analysis including Cardiotoxicity; Mutagenicity; BBB; Clinical Toxicity; GABA; VG Na^+.

Derivative Name	Cardiotoxicity	Mutagenicity	BBB	Clinical Toxicity	GABA	VG Na^+
SB-1	I-0.93	I-0.68	A-0.97	A-0.60	I-0.71	I-0.61
SB-2	I-0.92	I-0.70	A-0.95	A-0.63	I-0.73	I-0.56
SB-3	I-0.92	I-0.71	A-0.96	A-0.62	I-0.73	I-0.55
SB-4	I-0.92	I-0.71	A-0.96	A-0.62	I-0.73	I-0.55
SB-5	I-0.92	I-0.70	A-0.92	A-0.63	I-0.71	I-0.56
SB-6	I-0.88	A-0.79	A-0.83	I-0.57	I-0.77	I-0.78
SB-7	I-0.86	I-0.65	A-0.96	A-69	I-0.60	I-0.66
SB-8	I-0.87	A-0.79	A-0.82	I-0.58	I-0.77	I-0.77
SB-9	I-0.89	A-0.80	A-0.83	I-0.58	I-0.75	I-0.75
SB-10	I-0.88	A-0.80	A-0.82	I-0.58	I-0.75	I-0.74

Table 6: Multiple interactions involving different amino acids; Hydrogen Bond; Electrostatic and Hydrophobic interactions.

SR.NO	3D	2D
SB-1	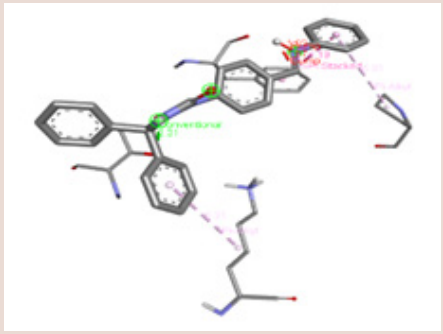	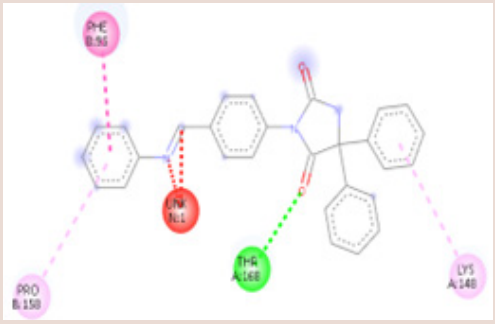
SB-2	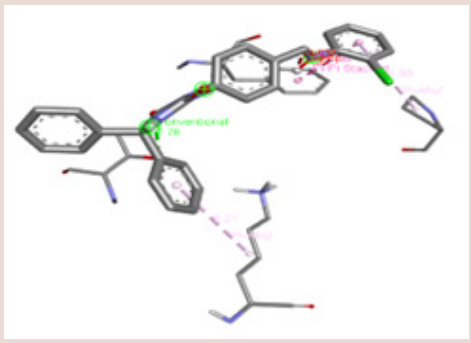	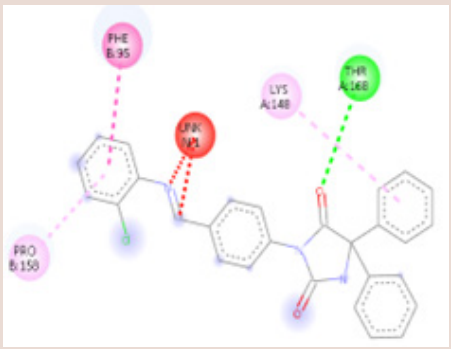
SB-3	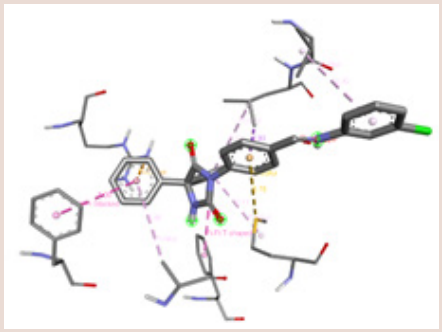	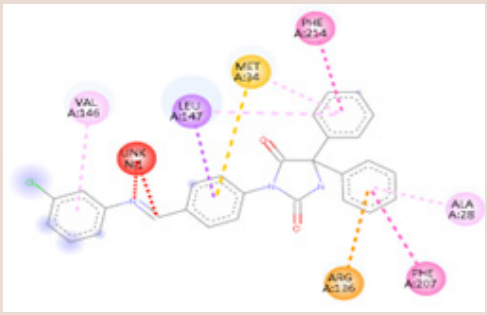
SB-4	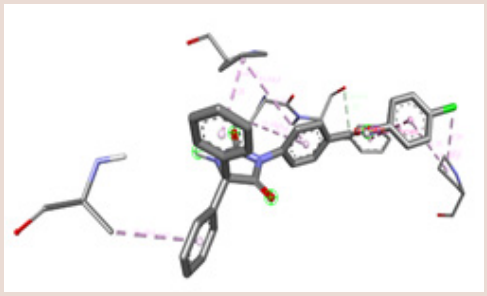	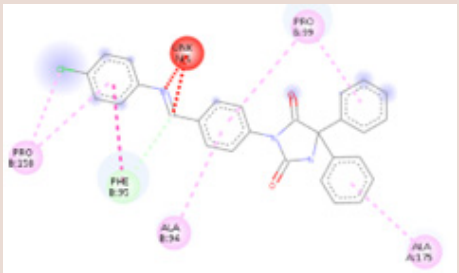
SB-5	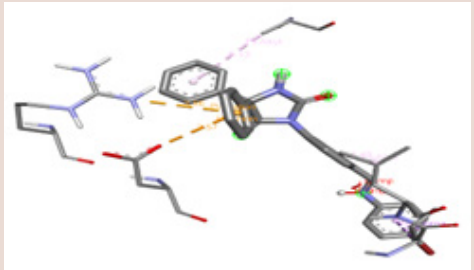	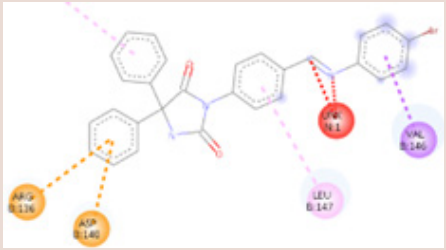

SR.NO	3D	2D
SB-6	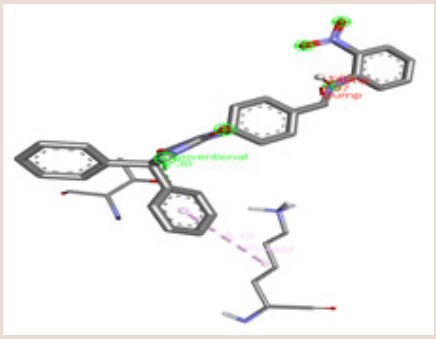	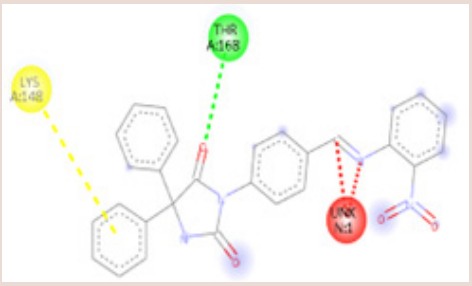
SB-7	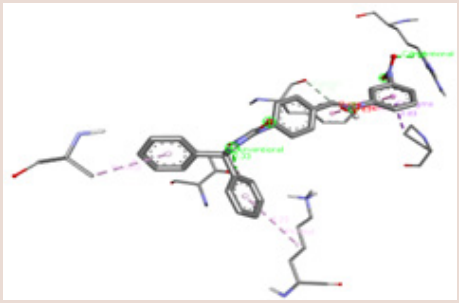	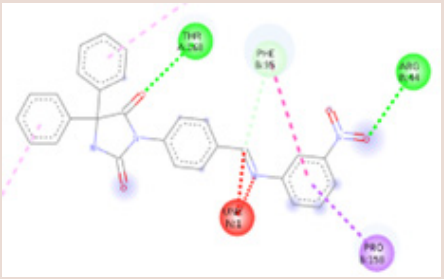
SB-8	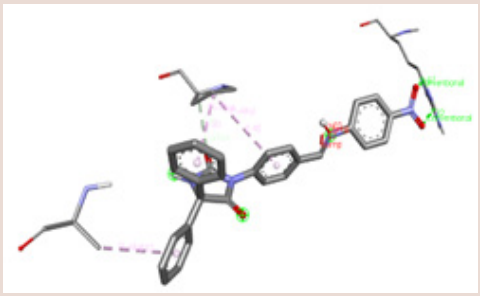	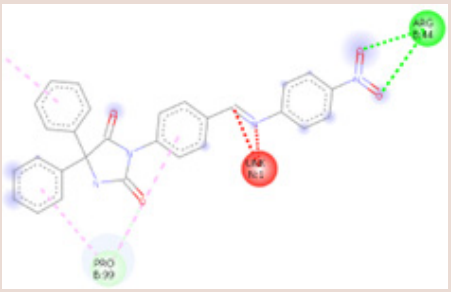
SB-9	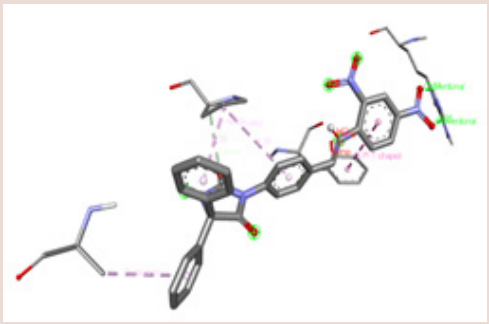	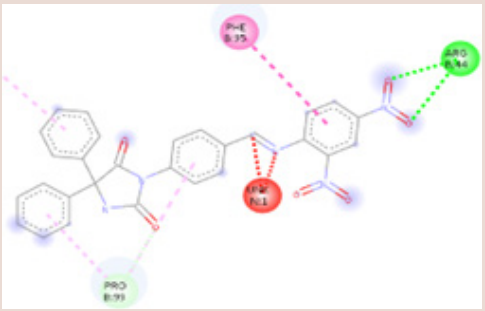
SB-10	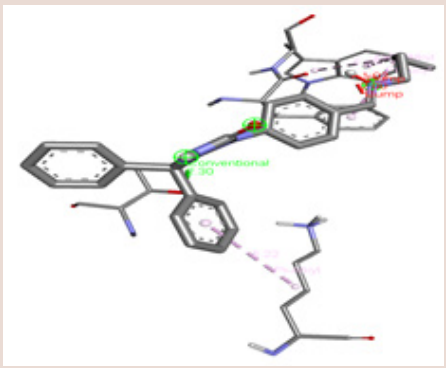	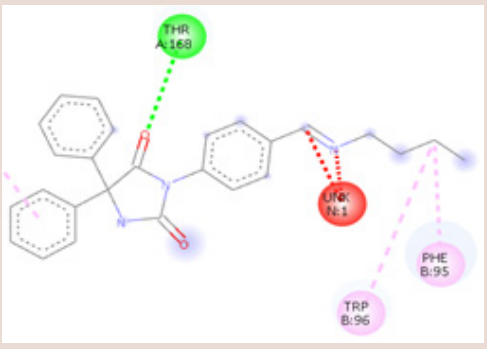

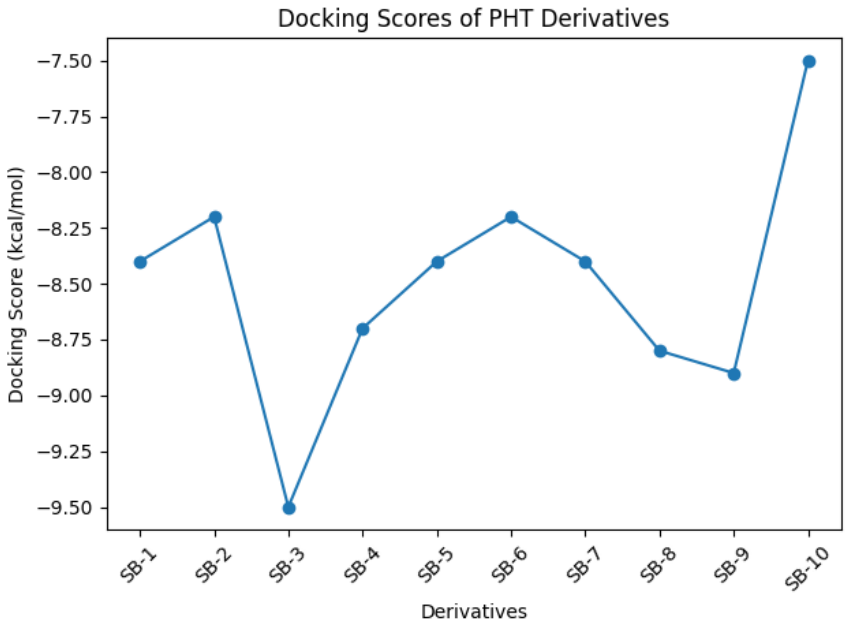

Figure 3: Molecular Docking Analysis of PHT Derivatives graph.

Table 7: Multiple interactions involving different amino acids; Hydrogen Bond; Electrostatic and Hydrophobic interactions.

Comp. Code	Name of Amino acid	Distance	Category	Types	Dock Score
SB-1	A:THR168: - PHE95 B:PRO158 A:LYS148	2.30558 4.19137 5.31175 5.21244	Hydrogen Bond Hydrophobic Hydrophobic Hydrophobic	Conventional Hydrogen Bond Pi-Pi Stacked Pi-Alkyl Pi-Alkyl	-8.4
SB-2	A:THR168N: B:PHE95 B:PRO158 A:LYS148	2.7769 4.03831 4.99048 5.20866	Hydrogen Bond Hydrophobic Hydrophobic Hydrophobic	Conventional Hydrogen Bond Pi-Pi Stacked Pi-Alkyl Pi-Alkyl	-8.2
SB-3	A:ARG136: A:LEU147: A:MET34:SD A:PHE207 - A:PHE214 - A:VAL146 - A:MET34 - A:LEU147 - A:ALA28	4.22273 3.80028 5.75932 5.06234 5.1546 5.42291 5.11002 5.19287 5.45567	Electrostatic Hydrophobic Other Hydrophobic Hydrophobic Hydrophobic Hydrophobic Hydrophobic Hydrophobic	Pi-Cation Pi-Sigma Pi-Sulfur Pi-Pi Stacked Pi-Pi T-shaped Pi-Alkyl Pi-Alkyl Pi-Alkyl Pi-Alkyl	-9.5
SB-4	N:UNK1: B:PHE95: B:PHE95 B:PRO158 B:ALA94 B:PRO99 B:PRO158 B:PRO99 A:ALA175	3.30089 4.68724 3.84145 5.08631 5.44761 4.94874 4.06392 4.63137	Hydrogen Bond Hydrophobic Hydrophobic Hydrophobic Hydrophobic Hydrophobic Hydrophobic Hydrophobic	Carbon Hydrogen Bond Pi-Pi Stacked Alkyl Pi-Alkyl Pi-Alkyl Pi-Alkyl Pi-Alkyl Pi-Alkyl	-8.7

Comp. Code	Name of Amino acid	Distance	Category	Types	Dock Score
SB-5	B:ARG136: B:ASP140: B:VAL146: B:LEU147 B:ALA28	3.95755 3.5733 3.47697 5.4262 5.12774	Electrostatic Electrostatic Hydrophobic Hydrophobic Hydrophobic	Pi-Cation Pi-Anion Pi-Sigma Pi-Alkyl Pi-Alkyl	-8.4
SB-6	A:THR168: A:LYS148	2.30183 5.13294	Hydrogen Bond Hydrophobic	Conventional Hydrogen Bond Pi-Alkyl	-8.2
SB-7	A:THR168: B:ARG44N: B:PHE95:O B:PRO158: B:PHE95 A:LYS148 A:ALA175	2.33322 2.54569 3.18918 3.88944 5.0188 5.2191 5.11218	Hydrogen Bond Hydrogen Bond Hydrogen Bond Hydrophobic Hydrophobic Hydrophobic Hydrophobic	Conventional Hydrogen Bond Conventional Hydrogen Bond Carbon Hydrogen Bond Pi-Sigma Pi-Pi Stacked Pi-Alkyl Pi-Alkyl	-8.4
SB-8	B:ARG44: B:ARG44 B:PRO99: N:UNK1 - B:PRO99 B:PRO99 - A:ALA175	2.6717 2.32134 3.33259 5.48517 4.00274 4.8221	Hydrogen Bond Hydrogen Bond Hydrogen Bond Hydrophobic Hydrophobic Hydrophobic	Conventional Hydrogen Bond Conventional Hydrogen Bond Carbon Hydrogen Bond Pi-Alkyl Pi-Alkyl Pi-Alkyl	-8.8
SB-9	B:ARG44: B:ARG44: B:PRO99: B:PHE95 B:PRO99 B:PRO99 A:ALA175	2.57378 2.35046 3.40696 4.92602 5.3895 4.0039 4.80288	Hydrogen Bond Hydrogen Bond Hydrogen Bond Hydrophobic Hydrophobic Hydrophobic Hydrophobic	Conventional Hydrogen Bond Conventional Hydrogen Bond Carbon Hydrogen Bond Pi-Pi T-shaped Pi-Alkyl Pi-Alkyl Pi-Alkyl	-8.9
SB-10	A:THR168: A:LYS148 B:PHE95 - B:TRP96 - B:TRP96 -	2.30369 5.21891 4.18483 5.25824 4.49481	Hydrogen Bond Hydrophobic Hydrophobic Hydrophobic Hydrophobic	Conventional Hydrogen Bond Pi-Alkyl Pi-Alkyl Pi-Alkyl Pi-Alkyl	-7.5

revealed that most derivatives comply with established criteria for oral drugs. Compounds SB-1 to SB-4 and SB-7 to SB-10 exhibited zero Lipinski violations, along with favorable bioavailability scores (0.55), indicating strong potential for oral administration. Conversely, SB-5 and SB-6 showed multiple rule violations and reduced bioavailability scores (0.17), suggesting the need for structural refinement. The toxicity prediction analysis provides encouraging insights into the safety profile of the compounds. All derivatives were predicted to be non-cardiotoxic, which is critical for CNS drugs. Most compounds were also non-mutagenic, although SB-6, SB-8, SB-9, and SB-10 showed moderate mutagenicity predictions, warranting further experimental

validation. Importantly, none of the compounds exhibited significant interaction with GABA receptors or voltage-gated sodium channels in toxicity models, indicating a lower risk of neurotoxicity or ion channel-related adverse effects. The molecular docking analysis revealed strong binding affinities of all derivatives toward the target protein, with docking scores ranging from -7.5 to -9.5 kcal/mol. Among the series, SB-3 demonstrated the highest binding affinity (-9.5 kcal/mol), which can be attributed to its diverse interaction profile, including electrostatic interactions (Pi-cation), hydrophobic contacts, π-π stacking, and π-alkyl interactions. These interactions significantly enhance ligand stabilization within the active site. Compounds SB-8 and SB-9 also exhibited strong binding affinities (-8.8 and -8.9 kcal/mol, respectively), supported by multiple hydrogen bonds with key residues such as ARG44. Hydrogen bonding interactions, particularly with residues like THR168 and ARG44, were observed across several derivatives and play a critical role in binding specificity and stability. Hydrophobic interactions involving residues such as PHE95, PRO158, and LEU147 further contributed to ligand stabilization. The docking results align well with the physicochemical and ADME findings, reinforcing the potential of SB-3, SB-8, and SB-9 as lead candidates. Notably, SB-3 stands out due to its superior binding affinity and diverse interaction network, while SB-8 and SB-9 demonstrate strong hydrogen bonding and favorable pharmacokinetic properties.

CONCLUSION

In conclusion, the present study successfully demonstrates the potential of PHT derivatives as promising anticonvulsant agents through comprehensive *in silico* analysis. The integration of physicochemical, pharmacokinetic, toxicity, and molecular docking studies highlights several key findings. Compounds SB-1 to SB-5 and SB-7 exhibited favorable drug-like properties, including optimal lipophilicity, high gastrointestinal absorption, and BBB permeability, making them suitable candidates for CNS activity. Among all derivatives, SB-3 emerged as the most promising lead compound, demonstrating the highest binding affinity and a diverse interaction profile within the active site of the target protein. Compounds SB-8 and SB-9 also showed strong potential due to their high docking scores and stable hydrogen bonding interactions. However, certain derivatives, particularly SB-6, displayed limitations in terms of permeability and pharmacokinetic properties, indicating the need for further structural optimization. While toxicity predictions suggest an overall favorable safety profile, the observed mutagenicity in some compounds and CYP450 inhibition highlights the importance of further *in vitro* and *in vivo* validation studies. Future research should focus on experimental validation, structure optimization, and pharmacodynamic studies to confirm the therapeutic efficacy of these compounds. In this research paper, provides valuable insights into the rational design of novel anticonvulsant agents and establishes a strong foundation for the development of next-generation sodium channel inhibitors for epilepsy treatment.

ACKNOWLEDGEMENT

The authors are thankful to Pravara Rural College of Pharmacy, Pravaranagar.

ABBREVIATIONS

ADME: Absorption, distribution, metabolism, and excretion; **BBB:** Blood-brain barrier; **CNS:** Central nervous system; **CYP:** Cytochrome P450; **CYP1A2:** Cytochrome P450 1A2; **CYP2C19:** Cytochrome P450 2C19; **CYP2C9:** Cytochrome P450 2C9; **CYP2D6:** Cytochrome P450 2D6; **CYP3A4:** Cytochrome P450 3A4; **GI:** Gastrointestinal; **HBA:** Hydrogen bond acceptor; **HBD:** Hydrogen bond donor; **Log Kp:** Logarithm of skin permeation coefficient; **LogP:** Logarithm of octanol-water partition coefficient; **MW:** Molecular weight; **PSA:** Polar surface area; **SA Score:** Synthetic accessibility score.

CONFLICT OF INTEREST

The authors declare that there is no conflict of interest.

REFERENCES

Acharjee, N., and Das, S. (2021). *In silico* drug design approaches in epilepsy research. Journal of Molecular Graphics and Modelling, 104, 107847. https://doi.org/10.1016/j.jmgm.2020.107847

Berman, H. M., Westbrook, J., Feng, Z., Gilliland, G., Bhat, T. N., Weissig, H., Shindyalov, I. N., and Bourne, P. E. (2000). The Protein Data Bank. Nucleic Acids Research, 28(1), 235-242. https://doi.org/10.1093/nar/28.1.235

Benet, L. Z., Hosey, C. M., Ursu, O., and Oprea, T. I. (2016). BDDCS classification system in drug discovery. The AAPS Journal, 18(1), 11-21. https://doi.org/10.1208/s12248-015-9837-7

Brodie, M. J., and Dichter, M. A. (1996). Antiepileptic drugs. New England Journal of Medicine, 334(3), 168-175. https://doi.org/10.1056/NEJM199601183340307

Chen, A. Y., and Liu, L. F. (1994). DNA topoisomerases: Essential enzymes and lethal targets. Annual Review of Pharmacology and Toxicology, 34, 191-218. https://doi.org/10.1146/annurev.pa.34.040194.001203

DiMasi, J. A., Grabowski, H. G., and Hansen, R. W. (2016). Innovation in the pharmaceutical industry. Journal of Health Economics, 47, 20-33. https://doi.org/10.1016/j.jhealeco.2016.01.012

Ekins, S., Mestres, J., and Testa, B. (2007). *In silico* pharmacology for drug discovery. British Journal of Pharmacology, 152(1), 9-20. https://doi.org/10.1038/sj.bjp.0707306

Ghose, A. K., Viswanadhan, V. N., and Wendoloski, J. J. (1999). Drug-like properties. Journal of Combinatorial Chemistry, 1(1), 55-68. https://doi.org/10.1021/cc9800071

Gleeson, M. P. (2008). Generation of drug-like molecules. Journal of Medicinal Chemistry, 51(4), 817-834. https://doi.org/10.1021/jm701122q

Gohlke, H., and Klebe, G. (2002). Approaches to molecular recognition. Angewandte Chemie International Edition, 41(15), 2644-2676. https://doi.org/10.1002/1521-3773

Goodford, P. J. (1985). A computational procedure for docking. Journal of Medicinal Chemistry, 28(7), 849-857. https://doi.org/10.1021/jm00145a002

Hevner, R. F. (2016). Brain development and disorders. Journal of Child Neurology, 31(3), 274-283. https://doi.org/10.1177/0883073815590002

Hopkins, A. L. (2008). Network pharmacology. Nature Chemical Biology, 4(11), 682-690. https://doi.org/10.1038/nchembio.118

Jorgensen, W. L. (2004). The many roles of computation. Science, 303(5665), 1813-1818. https://doi.org/10.1126/science.1096361

Kwan, P., and Brodie, M. J. (2000). Early identification of refractory epilepsy. New England Journal of Medicine, 342(5), 314-319. https://doi.org/10.1056/NEJM200002033420503

Lipinski, C. A. (2004). Lead- and drug-like compounds. Drug Discovery Today, 9(8), 337-341. https://doi.org/10.1016/S1359-6446(04)03029-7

Lipinski, C. A., Lombardo, F., Dominy, B. W., and Feeney, P. J. (1997). Experimental and computational approaches. Advanced Drug Delivery Reviews, 23(1-3), 3-25. https://doi.org/10.1016/S0169-409X(96)00423-1

Lionta, E., Spyrou, G., Vassilatis, D. K., and Cournia, Z. (2014). Structure-based virtual screening. Current Topics in Medicinal Chemistry, 14(16), 1923-1938. https://doi.org/10.2174/1568026614666140929124445

Morris, G. M., Huey, R., Lindstrom, W., Sanner, M. F., Belew, R. K., Goodsell, D. S., and Olson, A. J. (2009). AutoDock4 and AutoDockTools4. Journal of Computational Chemistry, 30(16), 2785-2791. https://doi.org/10.1002/jcc.21256

Ng, P. W., and Henikoff, S. (2003). SIFT prediction method. Nucleic Acids Research, 31(13), 3812-3814. https://doi.org/10.1093/nar/gkg509

O'Boyle, N. M., Banck, M., James, C. A., Morley, C., Vandermeersch, T., and Hutchison, G. R. (2011). Open Babel. Journal of Cheminformatics, 3(1), 33. https://doi.org/10.1186/1758-2946-3-33

Pardridge, W. M. (2005). Blood-brain barrier drug targeting. Drug Discovery Today, 10(9), 611-619. https://doi.org/10.1016/S1359-6446(05)03454-7

Pires, D. E. V., Blundell, T. L., and Ascher, D. B. (2015). pkCSM method. Journal of Medicinal Chemistry, 58(9), 4066-4072. https://doi.org/10.1021/acs.jmedchem.5b00104

Rogers, D., and Hahn, M. (2010). Extended-connectivity fingerprints. Journal of Chemical Information and Modeling, 50(5), 742-754. https://doi.org/10.1021/ci100050t

Santos, R., Ursu, O., Gaulton, A., Bento, A. P., Donadi, R. S., Bologa, C. G., Oprea, T. I. (2017). Target validation in drug discovery. Nature Reviews Drug Discovery, 16(1), 19-34. https://doi.org/10.1038/nrd.2016.230

Sliwoski, G., Kothiwale, S., Meiler, J., and Lowe, E. W. (2014). Computational drug discovery methods. Pharmacological Reviews, 66(1), 334-395. https://doi.org/10.1124/pr.112.007336

Trott, O., and Olson, A. J. (2010). AutoDock Vina. Journal of Computational Chemistry, 31(2), 455-461. https://doi.org/10.1002/jcc.21334

Veber, D. F., Johnson, S. R., Cheng, H. Y., Smith, B. R., Ward, K. W., and Kopple, K. D. (2002). Molecular properties affecting bioavailability. Journal of Medicinal Chemistry, 45(12), 2615-2623. https://doi.org/10.1021/jm020017n

Cite this article: Bhure SS, Bhor RJ, Shirode AM, Jadhav PB, Anap HN, Gosavi AR, *et al*. Molecular Docking and ADMET Profiling of Hydantoin Derivatives Targeting Voltage-Gated Sodium Channel (PDB ID: 1N45) for Epilepsy Treatment. Asian J Biol Life Sci. 2026;15(2):353-65.